

Dynamic analysis on a buried horizontal double-layer SF-type liquid-storage tank by finite element method

X. Cheng*, L. Hu, W. Zhang

Key Laboratory of Disaster Prevention and Mitigation in Civil Engineering of Gansu Province, Lanzhou University of Technology, Lanzhou, 730050, PR China

D. Yu

Western Engineering Research Center of Disaster Mitigation in Civil Engineering of Ministry of Education, Lanzhou University of Technology, Lanzhou, 730050, PR China

*Email: chengxuansheng@gmail.com

ABSTRACT: To study the dynamic responses of a buried horizontal double-layer SF-type liquid-storage tank considering liquid-solid interaction, a three-dimensional finite element model of the double-layer buried horizontal liquid-storage tank is established, and the model is calculated and simulated by using FEM (finite element method). The results show that the double-layer buried horizontal SF-type liquid-storage tank is a composite multi-layer structure; thus, the dynamic responses of the inner layer, interlayer and outer layer are different under the same earthquake wave: the tank wall displacement of the interlayer is the maximum, whereas that of the outer layer is the minimum; the tank wall equivalent stress of the inner layer is the maximum, whereas that of the outer layer is the minimum; and the distributions of strain and velocity in the inner and outer layers are also different. The double-layer SF-type oil-storage tank has different dynamic response rules under the actions of the El-Centro wave and the Lanzhou wave. Compared with the El-Centro wave, the dynamic responses of the double-layer oil-storage tank are more significant under the action of the Lanzhou wave. The dynamic responses of the horizontal double SF tank are found to be closely related to the spectral characteristics of the seismic wave and exhibit different dynamic responses under different earthquakes.

KEYWORD: Double-layer liquid-storage tank, Finite element, Liquid-solid interaction, Earthquake response

1 INTRODUCTION

With the rapid development of the national economy and the petroleum chemical industry, petroleum, as the lifeline of the national economy, affects the national security, economy, military and plays a vital role in the development and progress of the country. As the basic equipment in the petroleum industry, the safety performance of buried oil-storage tanks under earthquake is attracting increasing attention. As the buried oil-storage tanks are buried underground, the environment and groundwater resources will be polluted greatly if the storage tanks are damaged in the earthquake; therefore, research on the earthquake response of buried horizontal double-layer SF-type storage tanks considering liquid-solid interaction is of great significance in practical engineering.

Over the years, many practical and simple FEMs (finite element methods) have been developed by many researchers regarding the mechanical properties of storage tanks, such as the FEM, the equivalent frame method, and the analysis method [1-3]. Using the additional mass method, the liquid-solid interaction was studied by Balendra et al. [4]; in this method,

the oil in the storage tank is essentially replaced by an additional mass. Assuming that the liquid was incompressible and considering the influence of gravity waves on the liquid surface, the effect of seismic action on the liquid sloshing height, tank wall displacement, equivalent stress and strain in the concrete liquid-storage structure was studied by Cheng et al. [5-8]. Based on the shear cantilever theory, the liquid-solid interaction vibration equation of a rectangular liquid-storage structure was established by Du et al. [9], and the coupled vibration characteristics of the full-liquid structure are obtained. El-Centro seismic waves were input simultaneously along the vertical and horizontal axes of ground vertical storage tanks, and using finite element software, the dynamic responses of the liquid-solid interaction system were analyzed by Kianoush et al. [10, 11]. Comparing the damage degrees of oil storage tanks with different isolation systems, the effect of each isolation system was analyzed by Shrimali et al. [12, 13]. A new formula for describing the additional mass was proposed by Liu et al. [14]. The liquid-solid interaction system was discretized and an asymmetric liquid-solid interaction finite element equation obtained by Xu et al. [15]. The seismic responses of large liquid-storage tanks were analyzed by Tan [16] from the perspectives of the FEM and

the analytical method to identify some rules of the seismic response and the difference between the two analytical methods. Based on the characteristics of the SF double-layer oil tank, reasonable simplifications and assumptions for the FRP outer layer, the interlayer, and the inner layer were made by Song et al. [17], and the separation model of the SF double-layer tank was established by using the FEM; next, finite element analysis of the model was carried out, and the stress characteristics of the FRP outer layer, interlayer, and inner layer were discussed.

Many scholars have performed detailed studies on the dynamic responses of liquid-storage structures from the aspects of theory, finite element, experiment, etc. and have also conducted comparative analyses on the vibration isolation effects of different isolation systems with liquid-storage structures. However, few studies have been performed on the earthquake responses of buried SF oil-storage structures, with most of these studies focused on large vertical anchorage and non-anchorage oil storage tanks and almost no studies considering buried horizontal double-layer oil tanks. Therefore, this paper, based on the studies of many scholars and considering the liquid-solid interaction effect, took the SF-type buried horizontal double-layer oil tank as a case study to establish the finite element model. The effects of seismic action on the liquid sloshing height, tank wall displacement, equivalent stress, strain and velocity of the SF-type buried horizontal double-layer oil tank were studied, the results of which can provide a theoretical basis for the seismic design of the SF-type buried horizontal double-layer oil tank.

2 LIQUID-SOLID INTERACTION ANALYSIS THEORY

2.1 Liquid-Solid Interaction Vibration System

The low-frequency vibration caused by liquid sloshing will affect oil-storage tank safety. Furthermore, in practical engineering, materials with light weight, high strength and thin walls are widely used in the manufacture of oil storage tanks. As a result, the interaction vibration of the structure and the liquid sloshing represents a problem that cannot be ignored. On the one hand, the interaction vibration will lead to system power instability; on the other hand, the large sloshing of the liquid in the container will exert a greater additional stress on the container, eventually resulting in the failure of the structure. Therefore, in this paper, the SF horizontal double-layer oil tank is studied. Assuming that the internal oil is an incompressible ideal fluid, considering the interaction vibration of the oil tank wall and the internal liquid, the seismic wave is input horizontally along the bot-

tom of the tank to study the dynamic responses of the horizontal double-layer SF oil tank under earthquake action. However, because the buried horizontal oil tank is a multi-layered structure buried in the ground and has a special shape, it is difficult to analyze the liquid-solid interaction problem under the earthquake load. The relationship shown in Fig. 1 can be used to describe the liquid-solid interaction problem.

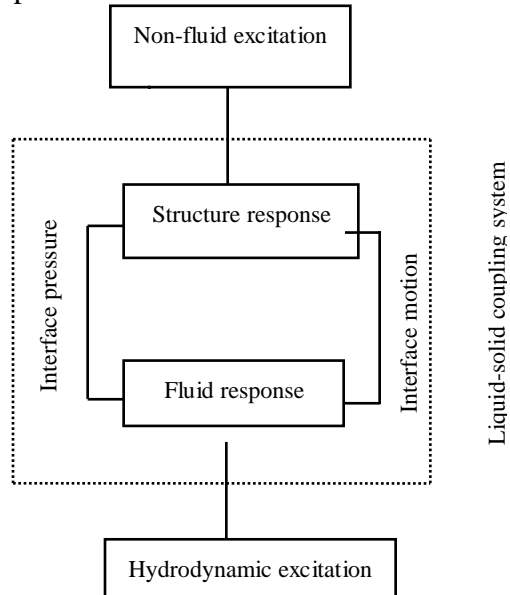


Figure 1 - Liquid-solid interaction vibration system

2.2 Liquid-Solid Interaction Motion Equations

In the liquid-solid interaction system, the equation of the solid domain always takes the displacement u_i as the basic unknown quantity, and the equation of the fluid domain usually adopts the flow field pressure p as the basic unknown; the finite element equation of the liquid-solid interaction system [18] is established according to the Galerkin method:

$$\begin{bmatrix} M_s & 0 \\ -Q^T & M_f \end{bmatrix} \begin{Bmatrix} a \\ p \end{Bmatrix} + \begin{bmatrix} K_s & \frac{1}{\rho_f} Q \\ 0 & K_f \end{bmatrix} \begin{Bmatrix} a \\ p \end{Bmatrix} = \begin{Bmatrix} F_s \\ 0 \end{Bmatrix} \quad (1)$$

where F_s is the buried tank external load vector, a is the tank node displacement vector, p is the pressure vector of the fluid node in the tank, and ρ_f is the fluid density.

The Eq. (1) is rewritten in symmetric form as follows:

$$\begin{bmatrix} M_s^s & E \\ E^T & M_f^s \end{bmatrix} \begin{Bmatrix} a \\ p \end{Bmatrix} + \begin{bmatrix} K_s^s & 0 \\ 0 & K_f^s \end{bmatrix} \begin{Bmatrix} a \\ p \end{Bmatrix} = \begin{Bmatrix} 0 \\ 0 \end{Bmatrix} \quad (2)$$

where
$$\mathcal{M}_s^{\circ} = M_s + \frac{1}{\rho_f} \phi K_f^{-1} \phi^T \quad ;$$

$$\mathcal{M}_f^{\circ} = \frac{1}{\rho_f} M_f K_f^{-1} M_f^T \quad ; \quad E = -\frac{1}{\rho_f} \phi K_f^{-1} M_f \quad ;$$

$$\mathcal{K}_s^{\circ} = K_s, \mathcal{K}_f^{\circ} = \frac{1}{\rho_f} M_f .$$

The characteristic equation of the liquid-storage tank considering liquid-solid interaction can be deduced as Eq. (2):

$$\left\{ \begin{bmatrix} \mathcal{K}_s^{\circ} & 0 \\ 0 & \mathcal{K}_f^{\circ} \end{bmatrix} - \omega^2 \begin{bmatrix} \mathcal{M}_s^{\circ} & E \\ E^T & \mathcal{M}_f^{\circ} \end{bmatrix} \right\} \begin{Bmatrix} a \\ p \end{Bmatrix} = 0 \quad (3)$$

Assuming that the liquid in the buried tank is an incompressible ideal fluid and the effect of free-surface gravity waves on the damping of the tank is neglected, Eq. (3) can be simplified as:

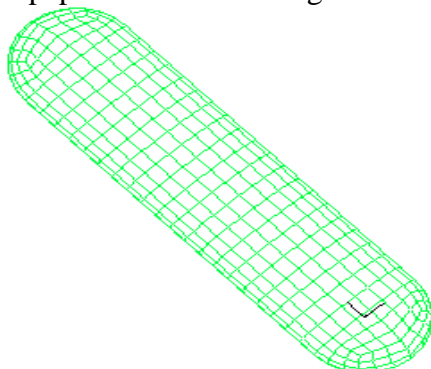
$$(M_s + M_s') \ddot{a} + K_s a = F_s \quad (4)$$

where M_s' represents the force of tank fluid on the tank wall, and
$$M_s' = \frac{1}{\rho_f} Q K_f^{-1} Q^T .$$

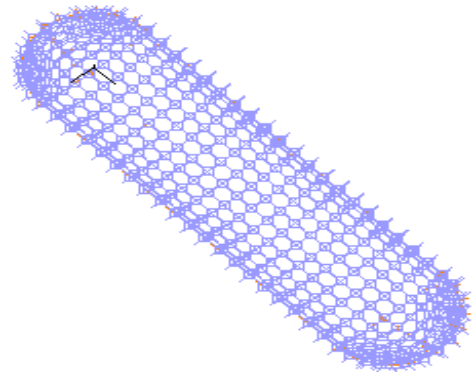
3 ANALYSIS MODEL AND SEISMIC WAVE

3.1 Spring Element Model

The soil-structure dynamic interaction effect involves the problem of the interactions of the soil, the structure and the contact surface at the soil-structure interface. These interactions represent a complex set of material nonlinear and geometric nonlinear problems. Therefore, many simplified analysis models and methods have been proposed to solve these problems, such as the lumped mass model, the spring element model and the whole finite element model; among these models, the spring element model has been generally accepted. Thus, the spring element is used to simulate the soil effect, and then, the structure-spring element calculation model is established. The structure- and spring-element models used in this paper are shown in Fig. 2.



(a) Structure element model

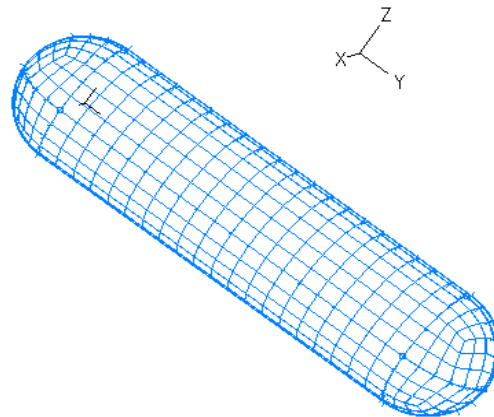


(b) Spring element model

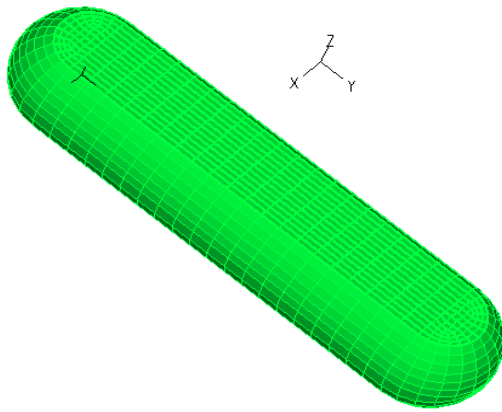
Fig. 2. Structure element models

3.2 Finite Element Structural Analysis Model

Selecting the buried double-layer SF-type oil tank as the calculation model with an inner diameter of 3.0 m and a middle cylinder length of 9.3 m, and with a hemispherical head at each end, the resulting model is a composite multi-layer structure. The inner layer is made of steel with a thickness of 8 mm, the small interlayer is made of hollow composite material with a thickness of 2.5 mm, and the outer layer is made of glass fiber reinforced plastic (FRP) with a thickness of 6 mm. The oil level height is taken as 2.8 m. The steel inner layer and the FRP shell are each simulated by a shell element, the interlayer is simulated by a three-dimensional solid element for quick and easy model building (although the thickness is very small), and the internal fluid is simulated by a three-dimensional fluid element. The fluid surface is defined as the free surface, and the spring element is used to simulate the soil to establish the structural spring element calculation model, as shown in Fig. 3.



(a) Oil storage tank



(b) Liquid

Fig. 3. Analysis model

3.3 Calculation Parameters

The horizontal double-layer SF-type tank is composed of the inner layer, inter layer and outer layer; thus, the tank is a composite structure in essence, and the material of each layer is different, resulting in a great difference in the material properties of each layer. To facilitate the calculation, assumptions

must be made for each layer of material [19]. The inner layer of the SF horizontal double-layer tank is made of steel, with the generally adopted yield strength of steel of 235 MPa; therefore, in the FEM, it is assumed that the inner layer is a bilinear plastic material (Bilinear). The FRP shell is a short-cut fiber-reinforced composite material, and the short fibers are two-dimensionally randomly distributed in the matrix; thus, the FRP shell is assumed to be an isotropic elastic material. The inter layer (which has a small thickness) serves two primary functions: one is to play a supporting role, and the other is to transfer the internal force of the FRP shell to the steel inner layer; because the inter layer has little influence on the structural strength, it is assumed that the inter layer is also an isotropic elastic material. The internal fluid is modeled using the 3D potential fluid (Potential-base Fluid) model, and only the bulk modulus and density of the material are defined.

Table 1. Specific parameters of each layer of material

Material category	Bulk modulus (Pa)	Elastic modulus (Pa)	Poisson's ratio (μ)	Density (kg/m^3)	Yield strength (Pa)
Inner layer	--	2.1×10^{11}	0.30	7850	3.45×10^8
Interlayer	--	3.5×10^4	0.35	850	—
Shell	--	7.0×10^5	0.36	860	—
Liquid	2.1×10^9	--	--	1000	—

3.4 Modal Analysis

The dynamic responses of double-layer SF tanks are related to the spectral characteristics of the seismic waves. The liquid sloshing and the natural frequency of the structure are first obtained through modal analysis and are then compared with the frequency

of the seismic waves to determine whether there will be a resonance phenomenon that adversely affects the structure. The first 10-order frequencies of the double-layer tank are shown in Table 2, and the first 10-order frequencies of liquid sloshing are shown in Table 3.

Table 2. The first 10-order frequencies of the double-layer tank

Vibration mode	Frequency	Vibration mode	Frequency
1	23.879	2	25.832
3	44.214	4	45.886
5	47.716	6	56.243
7	70.978	8	71.978
9	72.863	10	78.724

Table 3. The first 10-order frequencies of liquid sloshing

Vibration mode	Frequency	Vibration mode	Frequency
1	0.558	2	0.574

3	0.599	4	0.631
5	0.667	6	0.706
7	0.741	8	0.746
9	0.759	10	0.769

From Table 2 and Table 3, the first 10-order frequencies of the double-layer tank are much higher than those of the liquid sloshing. The first-order translational period of the double-layer oil tank is approximately 0.04 s. The first-order sloshing period of the liquid is approximately 1.79 s, which is far from the predominant period and the average period of the seismic wave; thus, no resonance phenomenon occurs.

3.5 Seismic Wave

Existing studies on earthquake ground motion mainly focuses on the three ground motion parameters, namely, amplitude, spectral characteristics and duration, because the ground motion is a vibration released by the earthquake source, and thus has a set of different amplitudes and frequencies in a finite time. The amplitude, the frequency characteristics and the duration are described below.

(1) Amplitude of the ground motion: The amplitude of the ground motion is used to indicate the intensity of the ground motion and is usually expressed by peak values, such as peak displacement, peak velocity and peak acceleration. The magnitude of the peak reflects the maximum intensity of the ground motion during the earthquake, which can be used to directly determine the magnitude of the earthquake energy and the magnitude of the destructive force that the earthquake exerts on the structure.

(2) Spectral characteristics: The spectral characteristics are used to represent the responses of structures with different natural vibration periods to earthquake-generated vibrations. In earthquake resistant engineering, the spectrum of ground motions is usually expressed by the response spectrum. The response spectrum $S(T, \zeta)$ is usually defined as follows: for a series of single freedom systems with the same damping ratio, the relationship between the natural vibration period and maximum reaction absolute value is $S(T, \zeta)$.

(3) Duration: Previous earthquake damage has shown that the duration of ground motion is also one of the main factors that affect the structural damage. In general, the longer the duration of the earthquake is, the greater the probability of permanent deformation of the structure. For the seismic designs of general civil buildings or industrial buildings, only

considering the amplitude of the earthquake can meet the design requirements; however, for special projects and important functional buildings, the duration of ground motion must be considered in seismic designs.

To study the earthquake responses of liquid-solid interaction regarding the buried horizontal double-layer tank, the acceleration time history of seismic waves is used for easy loading, and the requirements of amplitude, spectral characteristics and duration of seismic motion are also considered. Therefore, in this paper, the dynamic analysis of the buried horizontal double-layer oil tank using the El-Centro seismic wave of the United States in 1940 is conducted. The corresponding acceleration time history curve of the earthquake is shown in Fig. 4. Through the analysis of the earthquake, the predominant period and average period are 0.56 s and 0.56974 s, respectively, and the seismic wave record duration is 30 s. The seismic waves are input along the Y direction of the buried horizontal double-layer SF-type tank.

4 EARTHQUAKE RESPONSE ANALYSES

4.1 Liquid Sloshing Height

The fortification intensity 8 of the El-Centro seismic wave is input along the Y direction of the buried horizontal double-layer SF-type oil tank, the buried depth is taken as 1.9 m, and the liquid level height is taken as 2.8 m. The liquid sloshing height in the oil tank is shown in Fig. 4.

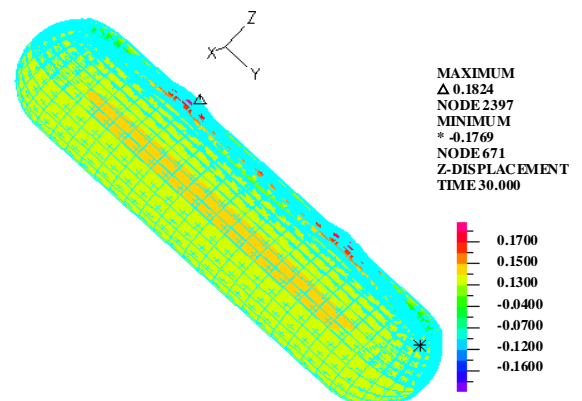


Fig. 4. Liquid sloshing height

When the liquid level in the tank is taken as 2.8 m, it can be seen from Fig. 4 that under the earthquake action, the maximum liquid sloshing height in the tank is 0.182 m, which occurs because the double tank is a closed structure, and the liquid sloshing will be limited by the upper tank wall.

4.2 Tank Wall Displacement

The fortification intensity 8 of the El-Centro seismic wave is input along the Y direction of the SF-type buried horizontal double-layer oil tank, the buried depth is taken as 1.9 m, and the liquid level height is taken as 2.8 m. The resulting tank wall displacement is shown in Fig. 5.

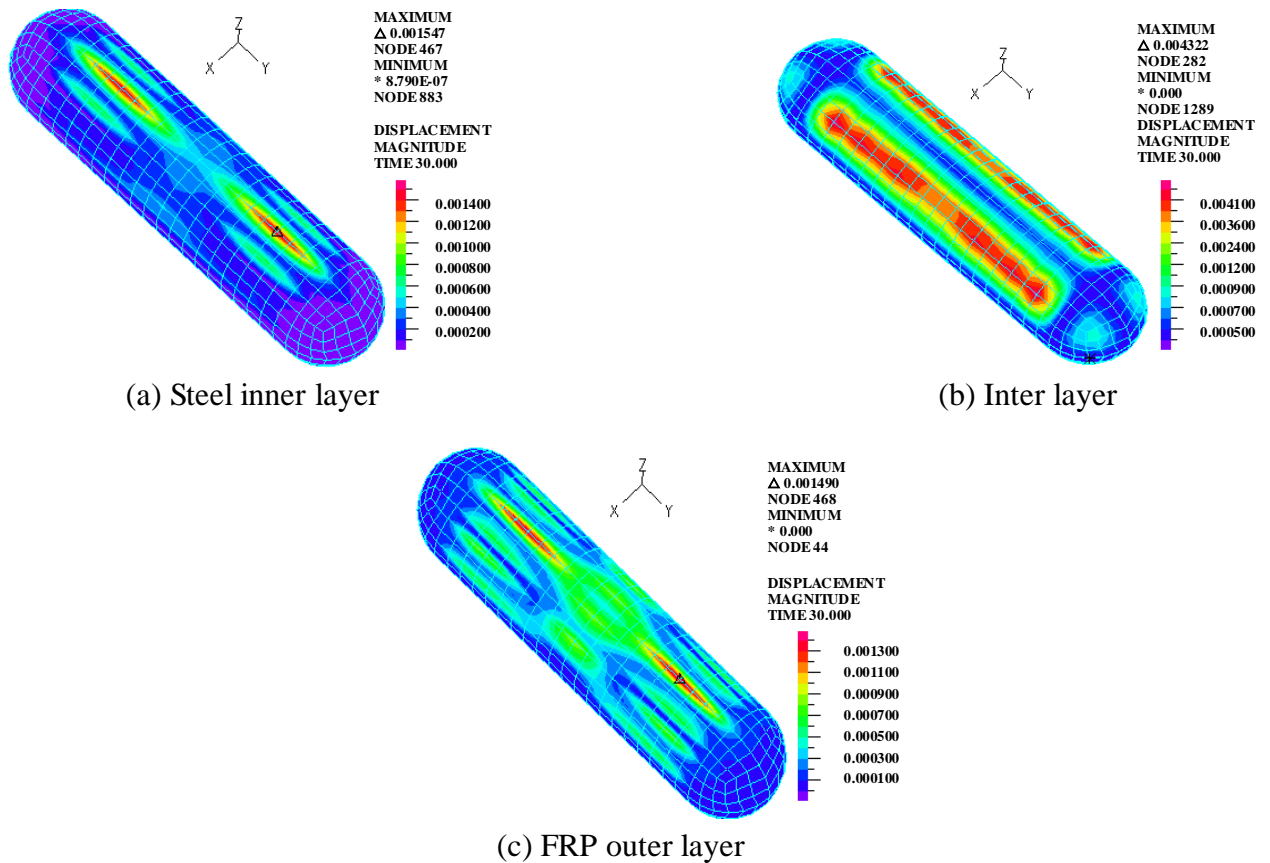


Fig. 5. Tank wall displacement

The peak values of the buried horizontal double-layer SF-type tank wall displacement are shown in Table 4.

Table 4. Peak values of the tank wall displacement /m

Tank wall	Inner layer	Interlayer	FRP outer layer
Displacement peak	0.001547	0.004322	0.001490

Fig. 5 shows that under the action of an earthquake, the displacements of the inner layer, the interlayer and the outer layer of the double-layer oil tank all exhibit a symmetrical phenomenon, and the displacement peak appears at the top of the tank wall. Table 4 also shows that the displacement of the interlayer is the maximum, followed by the displacement of the steel inner layer, and the displacement of the FRP outer layer is the minimum.

To more intuitively explain the difference between the steel inner layer and outer layer displacements under the action of 8-degree earthquake, the key node 383 is taken in the middle of the top of the steel inner middle cylinder, and the key node 4 is taken at the left head top. Correspondingly, the key node 384 is taken at the middle of the top of the outer middle cylinder, and the key node 41 is taken at the left head top. The displacement time history curves of the key nodes in the 6 s before the earthquake is shown in Fig. 6 and Fig. 7.

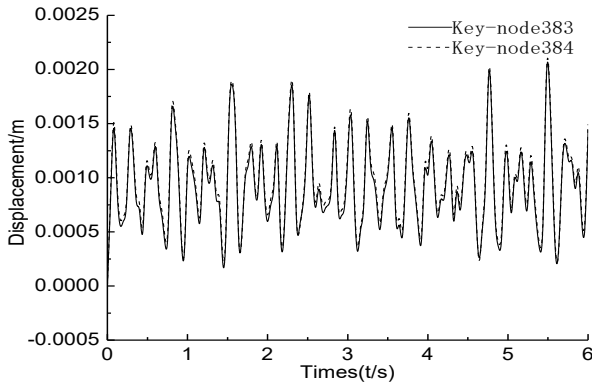


Fig. 6. Displacement time history curves of key nodes 383 and 384

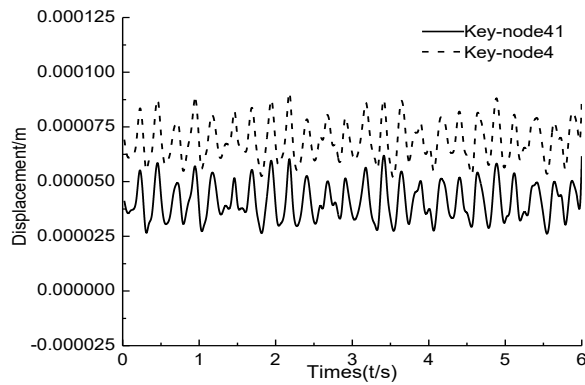


Fig. 7. Displacement time history curves of key nodes 4 and 41

According to Fig. 6, the displacement of the inner and outer layers of the upper half of the middle cylinder of the buried double-layer SF-type oil tank all produce larger displacements, and the displacement values of the inner and outer layers are close. Fig. 7 shows that although the displacements of the inner and outer layers of the upper half of the left and right hemispherical heads of the SF-type buried horizontal double-layer oil tank are both small, the displacements of the inner and outer layers are quite different, with the displacement value of the steel inner layer being greater than the displacement value of the outer layer.

4.3 Effective Stress

The 8-degree El-Centro seismic wave is input along the Y direction of the SF-type buried horizontal double-layer oil tank, the buried depth is taken as 1.9 m, and the liquid level height is taken as 2.8 m. The equivalent stress of the double-layer tank wall is shown in Fig. 8. The differences of the equivalent stress among the steel inner layer, the interlayer and the FRP outer layer are shown in the figure.

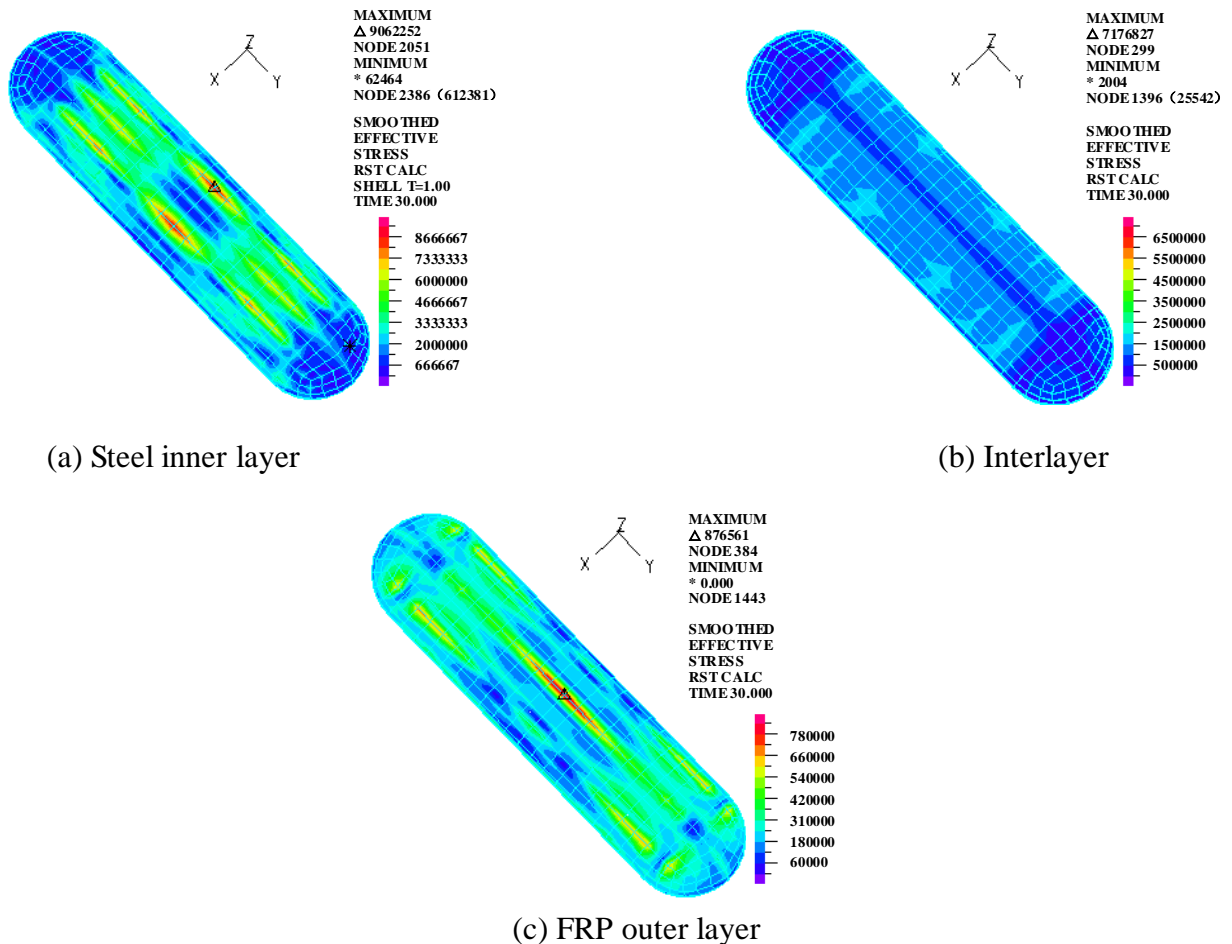


Fig. 8. Effective stress

The equivalent stress peak values of the buried horizontal double-layer SF-type oil tank wall are shown in Table 5.

Table 5. Peak value of tank wall effective stress

Tank wall	Inner layer	Interlayer	FRP outer layer
Peak value of equivalent stress	9062252	7176827	876561

When the liquid level in the tank is 2.8 m and the buried depth is 1.9 m, Fig. 8 shows that when the SF-type buried horizontal double-layer tank is under the action of an earthquake, the equivalent stress distributions of the steel inner layer, interlayer and FRP outer layer each show a symmetrical phenomenon. The equivalent stress peak value of the steel inner layer appears in the left and right sides of the central part of the middle cylinder, and the peak of the equivalent stress of the FRP outer layer appears in the central position of the upper part of the middle

cylinder. Furthermore, Table 5 shows that the equivalent stress peak value of the steel inner layer is far greater than the peak equivalent stress of the FRP outer layer, being more than 10 times different; that is, for the three walls of the oil tank, the force is mainly borne by the steel inner layer. Therefore, under the action of an earthquake, the steel inner layer may be the first to be damaged; as a result, the seismic measures of the steel inner layer should be improved.

4.4 Strain Analysis

The fortification intensity 8 of the El-Centro seismic wave is input along the Y direction of the SF-type buried horizontal double-layer oil tank, the buried depth is taken as 1.9 m, and the liquid level height is taken as 2.8 m. The tank wall strain of the double-layer tank is shown in Fig. 9.

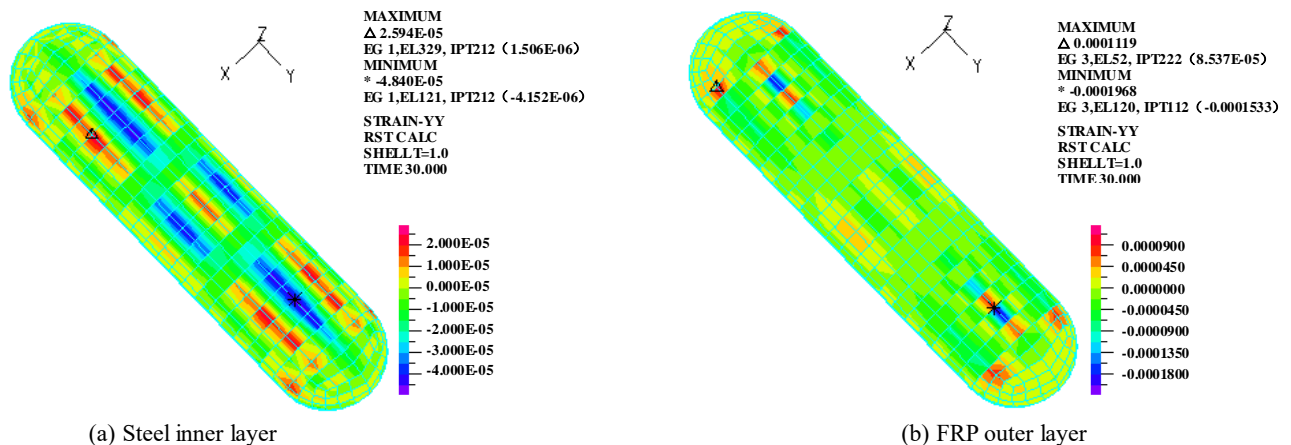


Fig. 9. Tank wall strain

Fig. 9 shows that the strain distribution of the inner layer in the Y direction mainly follows the following trends: The negative strain is mainly distributed in the middle of the upper part of the tank wall and the lower part of the tank wall, while the positive strain is mainly distributed on the left and right sides of the upper part of the tank wall, and the maximum strain value is 2.594×10^{-5} Pa. The strain distribution of the outer layer in the Y direction is as follows: Negative strain is mainly distributed in the middle cylinder, the positive strain is mainly distributed in the upper part of both ends of the head, and the maximum value is 1.119×10^{-4} Pa.

5 CASE ANALYSIS

For further study, the Lanzhou wave is input into a project of Lanzhou city to study the earthquake re-

sponse of liquid-solid interaction regarding the SF-type horizontal double-layer oil tank under different earthquakes; the duration of the Lanzhou wave is taken as 16.58 s. According to the Code for seismic design of buildings (GB50011-2010), the seismic fortification intensity in Lanzhou is 8, and the basic design acceleration of ground motion is 0.20 g. Therefore, according to the code, the Lanzhou wave acceleration amplitude is adjusted to 0.20 g. The acceleration time history curve of the Lanzhou wave is shown in Fig. 10.

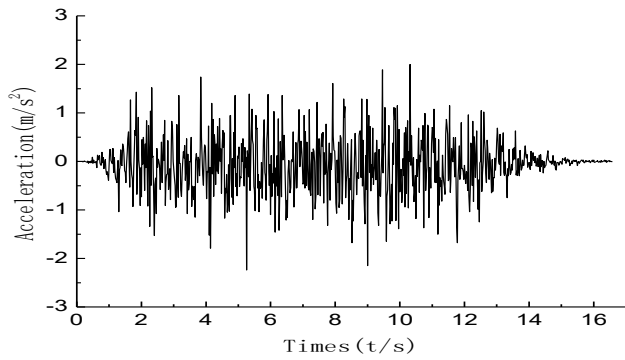


Fig. 10. Acceleration time history curve of the Lanzhou wave

5.1 Liquid Sloshing Height

The Lanzhou wave is input along the Y direction of the double-layer tank; after the finite element analysis, the sloshing height of the horizontal double-layer SF tank is obtained, as shown in Fig. 11.

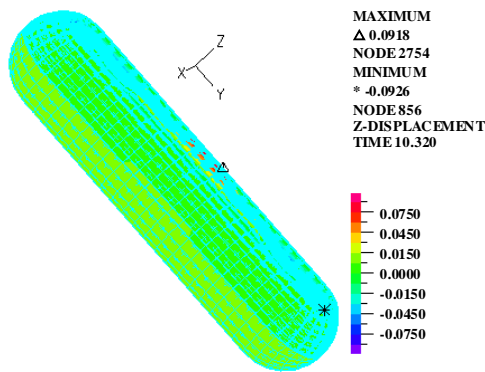


Fig. 11. Liquid displacement

According to the liquid displacement in the Z direction, when the liquid height in the oil tank is taken as 2.8 m and the Lanzhou wave is input along the Y direction of the buried horizontal double-layer oil tank, the maximum height of liquid sloshing is 0.0918 m, and the maximum height of liquid sloshing under the action of the El-Centro wave in the tank is 0.0824 m. The influence of the Lanzhou wave on the liquid sloshing height is found to be greater than that of the El-Centro wave.

5.2 Tank Wall Displacement

The Lanzhou wave is input along the Y direction of the double-layer tank; after the finite element analysis, the displacements of the SF horizontal double-layer tank wall are obtained, and then, the tank wall displacements under the El-Centro wave are compared and analyzed as shown in Table 6.

Table 6. Peak values of tank wall displacements (m)

Seismic waves	Steel inner layer	Interlayer	Outer layer
El-Centro wave	1.547×10^{-3}	4.322×10^{-3}	1.490×10^{-3}
Lanzhou wave	1.584×10^{-3}	8.648×10^{-3}	1.528×10^{-3}

According to Table 6, compared with the El-Centro wave, the tank wall displacement under the Lanzhou wave is larger. However, as with the El-Centro wave, the tank wall displacement still follows the trend that the maximum occurs in the interlayer, followed by the steel inner layer, and the smallest occurs in the outer layer. Moreover, the displacement

values of the steel inner layer and outer layer are similar.

5.3 Tank Wall Effective Stress

The Lanzhou wave is input along the Y direction of the double-layer tank. The effective stress of the buried horizontal double-layer SF tank wall is obtained, as shown in Fig. 12.

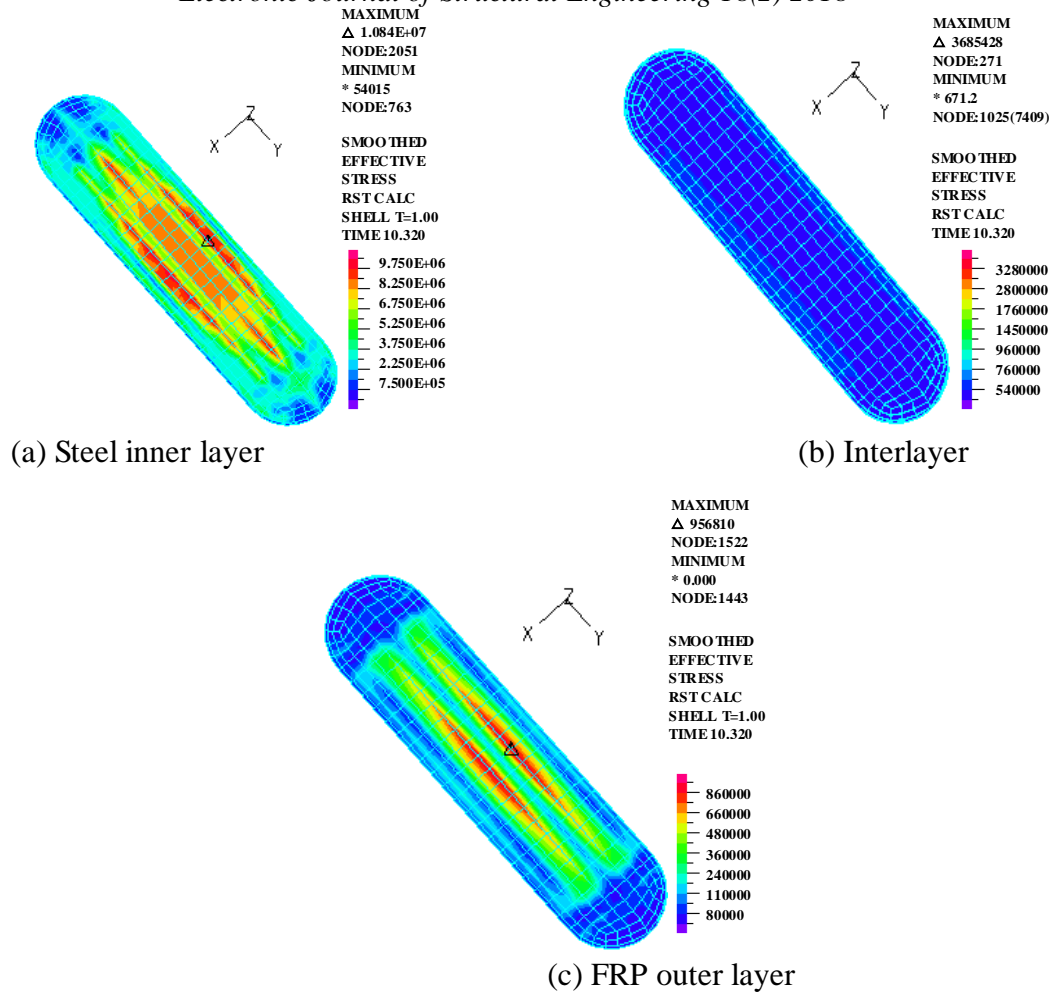


Fig. 12. Tank wall effective stress

The peak values of the tank wall effective stress extracted from Fig. 12 are shown in Table 7.

Table 7. Peak value of tank wall effective stress (Pa)

Seismic waves	Steel inner layer	Interlayer	Outer layer
El-Centro wave	9.062×10^6	7.177×10^6	8.766×10^5
Lanzhou wave	1.084×10^7	3.685×10^6	9.568×10^5

As seen from Table 7, compared with the El-Centro wave, the effective stresses of the steel inner layer and the outer layer under the Lanzhou wave are larger, but the effective stress of the interlayer is smaller. However, as with the El-Centro wave, the tank wall effective stress still follows the trend that the steel inner layer stress is the largest, followed by

the interlayer, and the smallest stress is in the outer layer.

5.4 Tank Wall Strain

The Lanzhou wave is input along the Y direction of the double-layer oil tank. After finite element analysis, the wall strains of the SF buried horizontal double-layer oil tank are obtained, as shown in Fig. 13.

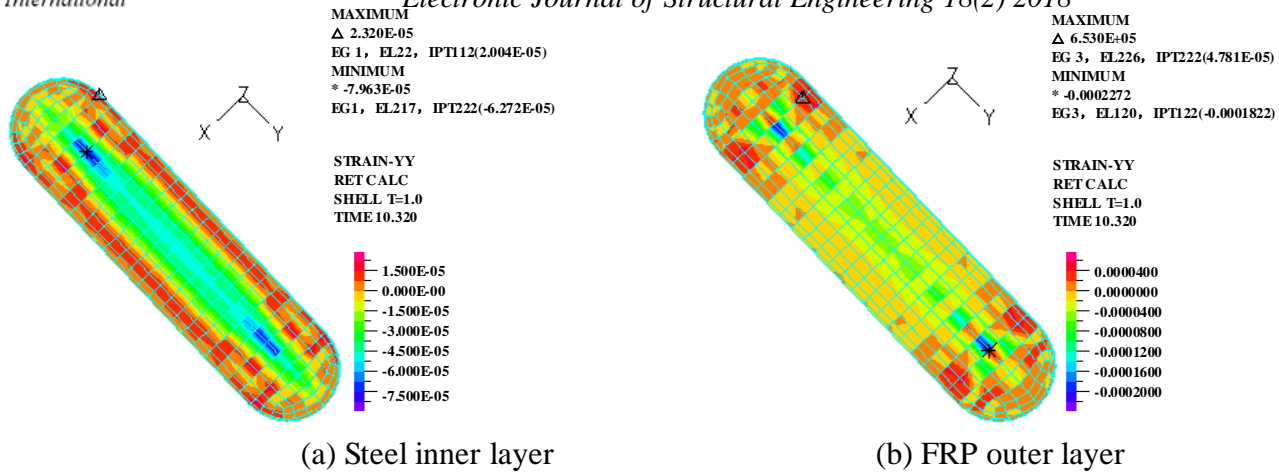


Fig. 13. Tank wall strains

From the analysis of Fig. 13, the strains distribution in the Y direction of the steel inner layer and the outer layer mainly obey the following rules. The normal strains are mainly distributed on the left and right sides of the upper part of the double-layer tank, and the maximum normal strain appears at the junction of the middle cylinder and the head, with a maximum value of 2.320×10^{-5} . The negative strains are mainly distributed near the central axis of the upper part of the middle cylinder, and the maximum negative strain appears in the position of the middle cylinder close to the head, with a maximum value of -7.963×10^{-5} . The normal strain of the outer layer is mainly distributed in the position of the upper part of the middle cylinder close to the head, and the maximum value is 6.530×10^{-5} . The negative strain is mainly distributed in the upper part of the middle cylinder near the central axis, and its maximum value is 2.272×10^{-4} . The distribution trend is basically the same as that under the action of the El-Centro wave, but the magnitudes of the positive and negative strains are different.

5.5 Result Analysis

In this section, the influences of different seismic waves (El-Centro wave and Lanzhou wave) on the dynamic response of the SF-type buried horizontal double-layer liquid-storage tank are analyzed. The main contents of the analysis include the liquid sloshing height, the tank wall displacement, and the tank wall stress and strain. The results show that the SF buried horizontal double-layer oil tank exhibits different dynamic responses under the actions of the El-Centro wave and the Lanzhou wave. Compared with the El-Centro wave, the liquid sloshing height, tank wall displacement, steel inner layer and outer layer effective stress, and steel inner layer and outer layer negative strain of the double tank under the action of the Lanzhou wave are larger; however, the

effective stress of the interlayer and the normal strains of the steel inner layer and the outer layer are smaller. It can be seen that the dynamic response of the SF horizontal double tank is closely related to the spectral characteristics of the seismic wave and is different under different earthquakes.

6 CONCLUSIONS

In this paper, for the case of the buried horizontal double SF-type tank, the finite element model considering liquid-solid interaction was established. The effects of the El-Centro wave on the liquid sloshing height, tank wall displacement, equivalent stress and strain of the buried horizontal double-layer SF-type oil tank were analyzed. Combined with the engineering example of Lanzhou, the earthquake responses of the liquid-solid interaction under different earthquakes were compared and analyzed. Based on the results, the following conclusions are obtained:

- (1) As the buried horizontal double-layer SF tank is a closed structure, the liquid sloshing height is less than the distance between the liquid level and the top. For the displacement of the tank wall, the peak values of the inner layer, the interlayer and the outer layer appear at the top of the tank wall; however, the peak value of the interlayer displacement is much larger than the displacements of the inner layer and the outer layer.
- (2) Under the action of an earthquake, the peak value of effective stress in the inner layer is much larger than that in the outer layer. Therefore, the steel inner layer is the main stress structure, and the seismic structure measures of the inner layer should be improved.
- (3) Because of the symmetrical structure of the buried horizontal double-layer SF-type oil tank, the strain distributions in the inner and outer layers ob-

viously show symmetry; however, the outer strain value is higher than the inner strain value.

(4) The horizontal double-layer SF-type oil tank shows different dynamic responses under the actions of the El-Centro wave and the Lanzhou wave. Compared with the El-Centro wave, the liquid sloshing height, the tank wall displacement, the steel inner layer and outer layer effective stresses, and the steel inner layer and outer layer negative strains of the double tank under the action of the Lanzhou wave are larger. However, compared with the El-Centro wave, the effective stress of the inter layer and the normal strains of the steel inner layer and the outer layer are smaller for the Lanzhou wave. The dynamic responses of the horizontal double SF tank are found to be closely related to the spectral characteristics of the seismic wave.

CONFLICT OF INTERESTS

The authors declare that there is no conflict of interests regarding the publication of this paper.

ACKNOWLEDGMENTS

This paper is a part of the National Natural Science Foundation of China (Grant number: 51478212), and a part of science and technology project in the Zhejiang Traffic Quality Supervision Bureau (Grant number: ZJ201602), and a part of science and technology project in China Railway 12th Bureau Group (Grant number: 14B-3).

REFERENCES

1. Li, Q. and Ma, X.R. Equivalent mechanical model for liquid sloshing in non-axisymmetric tanks. *Journal of Astronautics*, 2011, 32(2):242-249.
2. Cheng, X.S., Jing, W., et al. Dynamic pressure of concrete frame structure under a blasting demolition environment. *Electronic Journal of Geotechnical Engineering*, 2014, 19 (2014), Bund, Z7:17823-17837.
3. Cheng, X., Cao, L., Zhu, H. Liquid-solid interaction seismic response of an isolated over ground rectangular reinforced-concrete liquid-storage structure. *Journal of Asian Architecture & Building Engineering*, 2015, 14(1):175-180.
4. Balendra, T. Seismic design of flexible cylindrical liquid storage tanks. *Earthquake Engineering and Structure Dynamics*, 1982,10(3):477-496.
5. Cheng, X.S., Li, P.J., Zhu, H.Y., et al. The liquid-solid interaction seismic response of non-isolation overground rectangular reinforced-concrete liquid-storage structures. *China Civil Engineering Journal*, 2014, 47:42-47.
6. Cheng, X.S. and Du, Y.F. Vibration characteristic analysis of rectangular liquid-storage structures considering liquid-

- solid interaction on elastic foundation. *Engineering mechanics*, 2011, 28(2):186-192.
7. Cheng, X.S. Liquid-solid interaction vibration of reinforced concrete rectangular liquid-storage tanks. *Journal of China Coal Society*, 2009, 34(3):340-344.
8. Cheng, X.S. and Zheng, Y.R. Free vibration characteristic analysis of the elastic liquid-storage tanks based on the bending shearing model. *Journal of Chongqing University*, 2011, 34(12): 132-137.
9. Du, Y.F., Shi, X.Y., Cheng, X.S. Vibration of Reinforced Concrete Rectangular Liquid-storage Structures with Liquid-structure Interaction. *Journal of Gansu Sciences*, 2008.
10. Chen, J.Z., Kianoush, M.R. Seismic response of concrete rectangular tanks for liquid containings. *Canadian Journal of Civil Engineering*, 2005, 32(32):739-752.
11. Kianoush, M.R., Mirzabozorg, H., Ghaemian, M. Dynamic analysis of rectangular liquid containers in three-dimensional. *Canadian Journal of Civil Engineering*, 2006, 33(5):501-507.
12. Shrimali, M.K., Jangid, R.S. A comparative study of performance of various isolation systems for liquid storage tanks. *International Journal of Structural Stability & Dynamics*, 2011, 02(04):573-591.
13. Shrimali, M.K., Jangid, R.S. Seismic analysis of base-isolated liquid storage tanks. *Journal of Sound & Vibration*, 2004, 275(1-2):59-75.
14. Liu, H.Z., Li, Q., Zhuang, Z., et al. Development of added mass model and application to dynamic analysis of cylindrical tanks. *Engineering Mechanics*, 2005.
15. Xu, G. Dynamic characteristic analysis of liquid-filled tanks as a 3-d fluid-structure interaction system. *Acta mechanica sinica*, 2004, 36(3).
16. Tan, X.J. Seismic response analysis of fluid-structure interaction of large liquid storage tank. *Institute of engineering mechanics, China earthquake administration*, 2007.
17. Song, S.Q., Zhang, S.F., Zhang, Q.X. Finite element analysis on the structure strength of double-wall S&F oil tank. *Petrochemical Equipment Technology*, 2014.
18. Sun, L.M., Zhang, Q.H., Zhao, Y. The Modal Analysis of Cylindrical Container Filled with Fluid. *Journal of Zhengzhou University*, 2005, 26(2):89-91.
19. Wang, J. Research on Seismic Reaction of Large Liquid Storage Tanks. *Pressure Vessel Technology*, 2008.